60-GHz 3-D Cavity Bandpass Filter for V-Band Gigabit Wireless Systems

Gang Zhang, Jianpeng Wang, Hui Gu, and Xin Xu

Ministerial Key Laboratory of JGMT
Nanjing University of Science and Technology, Nanjing 210094, China
elegzhang@gmail.com, eejpwang@gmail.com, guhuinjust@gmail.com, xuxinnjust@gmail.com

Abstract ─ In this paper, a compact 60-GHz Three-Dimensional (3-D) SIW-based bandpass filter is presented using Low-Tmperature Co-fired Ceramic technology (LTCC). The filter is composed of four cavities. The coupling scheme is made up of three direct coupling and one cross coupling between the first and the fourth SIW cavities. By using the cross coupling technology and the cavity transformation property, two Transmission Zeros (TZs) are introduced outside the passband to increase the filtering selectivity. Both simulated and measured results are presented in good agreement.

Index Terms ─ 60-GHz, bandpass filter, compact, Low-Temperature Co-fired Ceramic (LTCC).

I. INTRODUCTION

As the demand for compact, low-loss Bandpass Filters (BPFs) increases in 60-GHz multigigabit-per-second wireless transceiver systems, integrating on-package cavity filters, based on the standard Substrate Integrated Waveguide (SIW) using multilayer Low-Temperature Co-fired Ceramic (LTCC) technology, has emerged as an attractive solution [1-5]. The LTCC based SIW cavity filters have a relatively high quality factor Q, a high power-handling capability compared to planar filter structures, and less interference from other circuits integrated in package.

Three LTCC bandpass filters with standard Chebyshev responses which exhibit poor out-of-band rejection are presented in [1,2,3]. Thus, to enhance the filtering selectivity, LTCC bandpass filters with quasi-elliptic responses which can introduce two transmission zeros outside the passband [4-5] are proposed. However, due to the mechanism of generating transmission zeros adopted in these designs, the circuit size is not compact. Therefore, the design of a LTCC millimeter-wave bandpass filter with a compact size and a high selectivity is meaningful.

The motivation of this paper is to propose a SIW-based LTCC 60-GHz bandpass filter, which can be fully integrated into miniaturized V-band LTCC transceiver modules. By introducing the cross-coupling mechanism and vertically coupled structure, a high filtering selectivity and a compact circuit size are both achieved. The design principles and processes are illustrated in detail. To verify the validity of the design method, both simulated and measured results are presented.

II. STRUCTURES AND DESIGN PROCESSES

Figure 1 shows the geometric configuration of the proposed SIW quasi-elliptic filter, consisting of four SIW cavity resonators which occupy substrate layers 2-5. And the filter is directly excited by the open-ended microstrip feedlines via coupling slots etched on the first/fourth cavity. The schematic topology of this filter is shown in Fig. 2, where k_{ij} represents the coupling coefficient between the i- and jth resonator cavity, while the solid and dashed lines indicate the main and cross-coupling paths, respectively. To achieve the quasi-elliptic function with a pair of attenuation poles at finite frequencies, it is essential that the signs of the coupling coefficients k_{12}, k_{23}, k_{34} should be opposite to k_{14}. However, it does not matter which

one of them is positive, as long as their signs are opposite. For convenience, it is assumed that k_{12}, k_{23}, k_{34} are positive while k_{14} is negative. To realize this negative coupling of k_{14}, the TE_{201}-mode is excited in cavity 3 using the cavity transformation property while the other three cavities are resonating at the TE_{101}-mode.
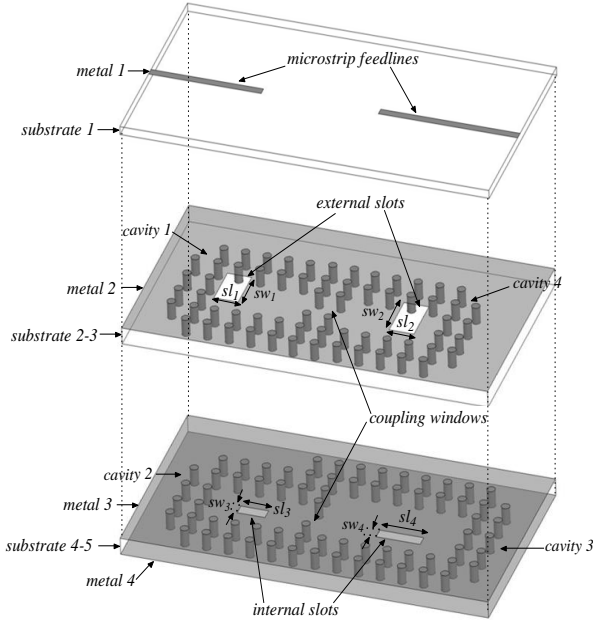

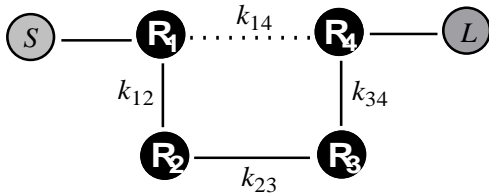Fig. 1. Geometric configuration of the proposed SIW cross-coupled filter.

Fig. 2. Equivalent schematic topology of the proposed SIW cross-coupled filter.

A. Circuit synthesis

The designed quasi-elliptic filter is centered at 59 GHz with 25 dB return loss in the passband while two normalized TZs are at ±2.27j. To achieve this design, we should firstly synthesize a low-pass prototype, which meets the given specification and determines an appropriate coupling matrix as well. Generally speaking, the synthesis of the filter has three steps. Firstly, the zeros and poles of the transfer function should be

obtained according to the specification of the filter. Secondly, generalized coupling matrix or generalized element values of the low-pass prototype can be obtained. Finally, we can calculate the design parameters by denormalizing the generalized element values. Based on the approach to the synthesis of cross-coupled resonators filter using the analytical gradient-based optimization technique [6], the generalized coupling matrix coefficients referred in Fig. 2 can be synthesized as shown in Table 1.

Table 1: Coupling matrix coefficients

Nonzero Entries	Normalizing Value
$M_{S1}= M_{S1}$	1.1413
$M_{12}= M_{12}$	0.9972
$M_{14}= M_{14}$	−0.1866
$M_{23}= M_{23}$	0.8375
$M_{34}= M_{34}$	0.9972
$M_{4L}= M_{4L}$	1.1413

The generalized coupling matrix is denormalized by using the following formula [7]:

$$k_{ij} = FBWM_{ij}, Q_e = 1/(FBWM_{S1}^2), FBW = BW/f_0. \quad (1)$$

Where FBW is the relative bandwidth, BW is the absolute bandwidth, and f_0 is the center frequency. Then the design parameters of the proposed filter are given as: k_{12}=0.0399, k_{23}=0.0334, k_{34}=0.0399, k_{14}=-0.0075, Q_e=19.2.

B. SIW cavity size

The SIW cavity resonator is constructed by a stacked LTCC substrate with a relative permittivity of 5.7, metal surfaces at the outer layers and via arrays. The SIW cavity size is determined by the corresponding resonant frequency using the following formula [8]:

$$f_{TE_{m0q}} = \frac{C_0}{2\sqrt{\varepsilon_r}} \sqrt{\left(\frac{m}{W_{eff}}\right)^2 + \left(\frac{q}{L_{eff}}\right)^2}, \quad (2)$$

$$L_{eff} = L - \frac{d^2}{0.95p}, W_{eff} = W - \frac{d^2}{0.95p}. \quad (3)$$

Where W and L are the width and length of the cavity, respectively. d and p are the diameters of metalized via-holes and center-to-center pitch between two adjacent via-holes. C_0 is the light velocity in vacuum. ε_r is the relative permittivity of the substrate.

C. External-coupling

In the proposed filter, the external quality factor Q_e can be controlled by the position and size of the coupling slots etched in the top metal layer (metal 2) of the cavities [9]. To determine the dimensions of the slots, the coupling slots are initially located at the position of a quarter of the cavity length and a short circuit is realized at the center of each slot by terminating the feedlines with $\lambda_g/4$ open stubs to maximize the coupling [10]. Then, the slots width is varied with constant $\lambda_g/4$ slot length, where λ_g is the guided wavelength at f_0. The external quality factor Q_e is calculated following the relationship below [7]:

$$Q_e = \frac{f_0}{\Delta f_{\pm 90^\circ}}. \tag{4}$$

Where $\Delta f_{\pm 90^\circ}$ is the frequency difference between the $\pm 90^\circ$ phase responses of S_{11}.

D. Internal coupling

The internal couplings are realized by broad-wall slots in different layers and a narrow-wall window at the same layer. The coupling coefficient of the broad-wall slot is affected by the length and position of the slot. To get strong direct coupling, the slot should be located as close to the sidewall of the cavity as possible. The coupling coefficient of the narrow-wall window is controlled by the separation degree between the via pair. All the internal couplings have been extracted (using full-wave simulation) according to the following equation [7]:

$$k_{ij} = \pm \frac{f_{c1}^2 - f_{c2}^2}{f_{c1}^2 + f_{c2}^2}. \tag{5}$$

In (5), f_{c1} and f_{c2} are defined as the high and low resonance frequencies, respectively. k_{ij} represents the coupling coefficient between the two SIW cavity resonators. The sign of the k_{ij} is dependent on the physical structure of the coupled resonators.

In addition, the principal mechanism of implementing the internal negative coupling coefficient between cavities 1 and 4, i.e., and k_{14} has been clarified below. As mentioned above, TE$_{201}$-mode is excited in cavity 3 using the cavity transformation property while the other three cavities are resonating at the TE$_{101}$-mode. The magnetic field distributions functioning in the proposed configuration is clearly depicted in Fig.

3. It is not difficult to find that the field direction within TE$_{101}$-mode cavity 4 determines the sign of the cross coupling k_{14}. This relationship is intrinsically determined by the TE$_{201}$-mode cavity 3 and the coupling slot location between cavities 3 and 4. As it is illustrated in Fig. 3, the magnetic fields between cavities 1 and 4 will be reversed when the coupling slot between cavities 3/4 is selectively located at the right half of cavity 3, resulting in the negative coupling coefficient [7]. Alternatively, if the coupling slot is arranged at the left half of cavity 3, the k_{14} will be positive, which can be further utilized to construct a filter with liner phase characteristics [11].
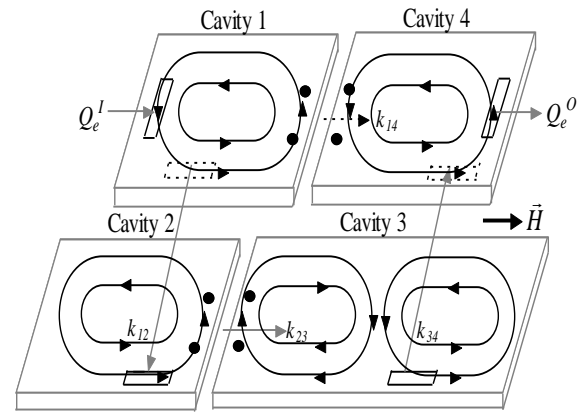

Fig. 3. Principal magnetic field patterns.

Based on the theory and process mentioned above, the initial dimensions of this filter could be deemed as optimal variables and they are well tuned to achieve the desired frequency response using High Frequency Structure Simulator (HFSSv12). The diameter of the metallic via hole is 0.15 mm and the space between two adjacent via holes is around 0.4 mm. The final dimensions of the filter illustrated in Figs. 1, 4 and 5 are the following: wm=0.13 mm, w1=1.3 mm, w2=1.3 mm, w3=1.46 mm, w4=1.54 mm, w5=1.71 mm, lt=4.29 mm, l1=1.93 mm, l2=1.97 mm, l3=1.95 mm, l4=2.73 mm, sp1=0.46 mm, sp2=0.575 mm, sp3=0.975 mm, sp4=0.905 mm, sw1=0.69 mm, sw2=0.84 mm, sw3=0.2 mm, sw4=0.2 mm, sl1=0.39 mm, sl2=0.46 mm, sl3=0.5 mm, sl4=0.82 mm, sh1=0.275 mm, sh2=0.275 mm, p1=0.66 mm, p2=0.74 mm, r1=1.135 mm, r2=0.965 mm, r3=0.965 mm, r4=0.965 mm, g1=0.375, g2=0.355 mm.
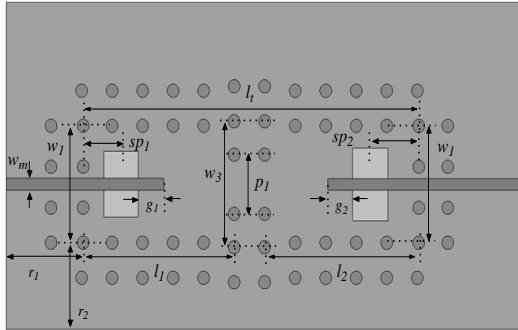
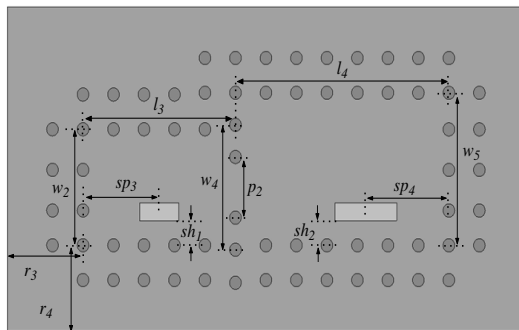Fig. 4. Geometric parameters of top view of the substrate layers 2-3 and metal 1.

Fig. 5. Geometric parameters of top view of the substrate layers 4-5.

III. FABRICATION AND MEASUREMENT

The designed filter is fabricated on LTCC substrate characterized by ε_r=5.7, tan δ=0.002, whose thickness is 0.1 mm. By connecting ZVA-75 frequency converts with a ZVA-50 vector network analyzer, we can convert the original frequency range of ZVA-50 vector network analyzer (10 MHz-50 GHz) to a new frequency range of 50-75 GHz. Therefore, the measurement frequency range can successfully cover the passband range of the filter through this method.

The photograph of the fabricated circuit is indicated in Fig. 6. Figure 7 shows the simulated and measured results of the proposed filter. The fabricated circuit exhibits an electrical size (including the CPW measurement pads) of 1.28 $\lambda_g \times$ 3.15 λ_g. The measured (simulated) center frequency of the passband is 59.48 GHz (58.85) with a 3-dB bandwidth of 2.1 (2.2) GHz. The minimum in-band insertion loss is 2.7 (2.2) dB approximately while the return loss is better than

14.7 (25.2) dB. Two TZs can be clearly identified at 56.5 and 61.6 GHz with rejection levels higher than 45 and 40 dB, respectively. These two TZs result in a high filtering selectivity. And the variation of the group time delay is smaller than 1% over 70% of the pass band around the central frequency as shown in Fig. 8, thus, implying good linearity in this bandpass filter. The shift of the centre frequency is mainly caused by the tolerance in the substrate permittivity at a high frequency and the misalignment between substrate layers. The higher insertion loss may be due to the loss tangent deviation at a high frequency, and the radiation loss from the 'thru' line that could not be well embedded because of the nature of the SOLT calibration and fabrication tolerance.
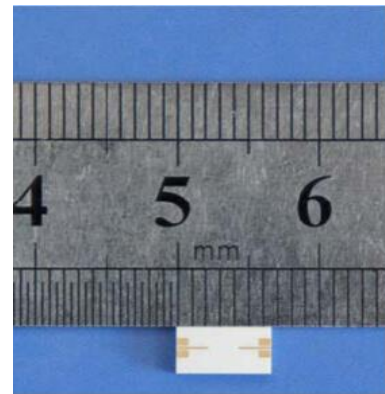

Fig. 6. Simulated and measured performances of the proposed filter including the insert photograph of the fabricated circuit.
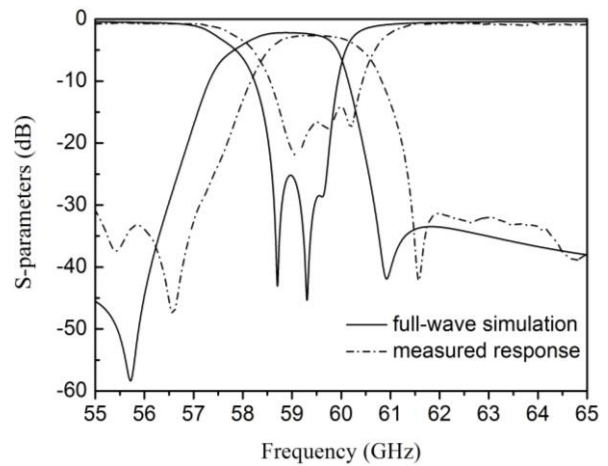

Fig. 7. Simulated and measured performances of the proposed filter of the fabricated circuit.
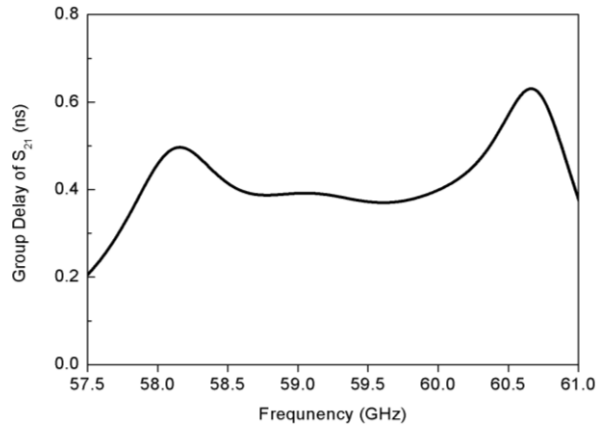
Fig. 8. The group time delay of the proposed filter.

IV. CONCLUSION

This paper presents a compact quasi-elliptic 60-GHz bandpass filter with a good performance using the LTCC technology. The design principle is given to reveal the realization of quasi-elliptic function responses. The proposed structures can be well integrated into miniaturized LTCC transceiver modules for V-band WPAN gigabit wireless communication systems.

ACKNOWLEDGEMENT

REFERENCES

[1] J. H. Lee, S. Pinel, J. Papapolymerou, J. Laskar, and M. M. Tentzeris, "Low-loss LTCC cavity filters using system-on-package technology at 60 GHz," *IEEE Trans. Microw. Theory Tech*., vol. 53, no. 12, pp. 3817-3824, December 2005.

[2] J. H. Lee, N. Kidera, G. DeJean, S. Pinel, J. Laskar, and M. M. Tentzeris, "A V-band front-end with 3-D integrated cavity filters/duplexers and antenna in LTCC technologies," *IEEE Trans. Microw. Theory Tech*., vol. 54, no. 7, pp. 2925-2936, July 2006.

[3] D. Dancila, X. Rottenberg, H. A. C. Tilmans, W. De Raedt, and I. Huynen, "57-64 GHz seven-pole bandpass filter substrate integrated waveguide (SIW) in LTCC," *2011 IEEE MTT-S Int. Microw. Symp. Dig*., pp. 200-203, September 2011.

[4] H. Chu, Y. X. Guo, and X. Q. Shi, "60 GHz LTCC 3D cavity bandpass filter with two finite transmission zeros," *Electron. Lett*., vol. 47, no. 5, pp. 324-326, March 2011.

[5] G. H. Lee, C. S. Yoo, Y. H. Kim, J. Y. Kim, Y. H. Park, J. G. Yook, and J. C. Kim, "A 60 GHz embedded SIW (substrate integrated waveguide) BPF considering the transition effect," *APMC Microw. Conf*., Singapore, pp. 1192-1195, December 2009.

[6] S. Amari, "Synthesis of cross-coupled resonator filters using an analytical gradient-based optimization technique," *IEEE Trans. Microw. Theory Tech*., vol. 48, no. 9, pp. 1559-1564, September 2000.

[7] J. S. Hong and M. J Lancaster, "Microstrip filters for RF/microwave applications," *Wiley*, New York, USA, 2001.

[8] Y. Cassivi, L. Perregrini, P. Arcioni, M. Bressan, K. Wu, and G. Conciauro, "Dispersion characteristics of substrate integrated rectangular waveguide," *IEEE Microw. Wireless Compon. Lett*., vol. 12, no. 2, pp. 333-335, February 2002.

[9] D. M. Pozar and D. H. Schaubert, "Microstrip antennas," *Piscataway, NJ: IEEE Press*, 1995.

[10] M. J. Hill, R. W. Ziolkowski, and J. Papapolymerou, "Simulated and measured results from a Duroid-based planar MBG cavity resonator filter," *IEEE Microw. Wireless Compon. Lett*., vol. 10, no. 12, pp. 528-530, December 2000.

[11] X. P. Chen, W. Hong, T. J. Cui, J. X. Chen, and K. Wu, "Substrate integrated waveguide (SIW) linear phase filter," *IEEE Microw. Wireless Compon. Lett*., vol. 15, no. 11, pp. 787-789, November 2005.

Gang Zhang received his B.S. degree in Electronics and Information Engineering from NJUST, Nangjing, China, in 2010. He is currently working in Electromagnetic Field and Microwave Technology with NJUST. His research interest is the design of miniaturized high performance microwave/millimeter-wave passive device and numerical methods in electromagnetics.

Jianpeng Wang received his M. Sc. and Ph. D. degrees from UESTC, Chengdu, China, in 2004, and 2007, respectively, both in Electronic Engineering. Since January 2008, he has been with the Ministerial Key Laboratory of JGMT, School of Electronic and Optical Engineering, NJUST, where he is currently an Associate Professor. His research interests include the high performance microwave/millimeter-wave passive components, circuits and systems realized on PCB, LTCC, etc.

Hui Gu received his B.S. degree in Electronics and Information Engineering from HNU, Huaian, China, in 2012. He is currently working towards his master degree in Communication and Information System with NJUST. His research interests include the high performance microwave/millimeter-wave passive device realized on PCB, LTCC, etc.

Xin Xu received his B.S. degree in Electromagnetic Field and Radio Technology from UESTC, Chengdu, China, in 2010. He is currently working towards his Ph.D. degree in Electromagnetic Field and Microwave Technology with NJUST. His research interests include the high performance microwave/millimeter-wave passive device realized on PCB, LTCC, etc.